Recoil corrections in heavy-ion-induced transfer*

A. J. Baltz and S. Kahana
Brookhaven National Laboratory, Upton, New York 11973
(Received 26 February 1974)

A perturbative approach for rapid calculation of recoil corrections to heavy-ion distorted-wave Born approximation has been developed. Without making either the local momentum approximation or the Hankel function approximation, we expand the final scattering wave function about $\vec{r}_f = \alpha \vec{r}_i$. We have modified the existing no-recoil code RDRC to include exactly the first-order term, allowing one to correct for both longitudinal and transverse recoil effects. Sample calculations have been performed, including an analytically solvable test case, plus the reactions ^{94}Mo(^{13}C, ^{12}C)^{95}Mo and ^{48}Ca(^{14}N, ^{13}C)^{49}Sc for which data have been taken and analyzed previously with RDRC. The relative α independence of the results argues strongly for convergence.

[NUCLEAR REACTIONS ^{48}Ca(^{14}N, ^{13}C), $E = 30$, 50, 70 MeV; ^{94}Mo(^{13}C, ^{12}C), $E = 48.5$ MeV; calculated proper first-order recoil DWBA. Q, L, and α (scaling parameter) dependence of calculated σ.]

I. INTRODUCTION

In the past several years the utility of distorted-wave Born approximation (DWBA) codes for analysis of heavy-ion-induced single-nucleon transfer data has been clearly demonstrated.[1-5] Existing heavy-ion DWBA codes employing the so-called "no-recoil" approximation have often been successful in reproducing transfer angular distributions, but are unlikely to be completely reliable for extracting spectroscopic strengths. There are undoubtedly situations for which an exact finite-range code[5] is necessary to permit meaningful evaluation of the direct-reaction mechanism. Unfortunately extensive use of such codes is rendered somewhat impractical by the large requirements of computer time and core memory.

In this paper we present an approximate method of calculating recoil effects in which the no-recoil calculation is seen as the zeroth order of a perturbation series. The form-factor localization implicit in the no-recoil approximation may then be exploited to obtain a rapid convergence for the series. The method is a series expansion[6] of the exit channel scattering distorted-wave function $\Psi^{(-)}(\vec{k}_f, \vec{r}_f)$ about the point $\vec{r}_f = \alpha \vec{r}_i$. Only the zeroth- and first-order terms in this expansion are retained. Nagarajan[7] has performed a similar expansion but with the additional approximation of replacing a bound-state wave function with a Hankel function, and of using a constant local wave number as the gradient operator in the first-order term. We make no such approximations and therefore our calculation approaches the exact finite-range result when higher-order terms are small.

In this paper we present an outline of the formalism required for our perturbative approach and apply the resulting code to two cases of existing data previously analyzed with the no-recoil code RDRC.[4] An extensive comparison with an exact integration of the finite-range formalism is in preparation.[8]

II. FORMALISM

The single-nucleon transfer reaction is of the form:

$$(A+n)+B \rightarrow A+(B+n),$$

where $A+n$ is the projectile and B the target nucleus. We use the coordinate system shown in Fig. 1. If spin-orbit interactions are ignored the exact DWBA cross section in the post representation may be written[4]

$$\frac{d\sigma}{d\Omega} = \frac{m_i m_f}{(2\pi\hbar^2)^2} \frac{k_f}{k_i} \left(\frac{2J_f+1}{2J_i+1}\right) (C_1{}^2S_1)(C_2{}^2S_2) \sum_{LM} \frac{(2L+1)}{(2l_1+1)} \left| W(l_2 j_2 l_1 j_1; \tfrac{1}{2} L) I^{l_1 l_2 LM} \right|^2, \tag{1}$$

with

$$I^{l_1 l_2 LM} = \sum_{m_1 m_2} \langle l_2 m_2 LM | l_1 m_1 \rangle \langle \Psi^{(-)}(\vec{k}_f, \vec{r}_f) \varphi^{l_2 m_2}_{j_2}(\vec{r}_2) | V(\vec{r}_1) | \varphi^{l_1 m_1}_{j_1}(\vec{r}_1) \Psi^{(+)}(\vec{k}_i, \vec{r}_i) \rangle, \tag{2}$$

where $\Psi^{(+)}(\vec{k}_i, \vec{r}_i)$, $\Psi^{(-)}(\vec{k}_f, \vec{r}_f)$ are the entrance and exit scattering wave functions while $\phi_{j_1}^{l_1 m_1}$, $\varphi_{j_2}^{l_2 m_2}$ are the wave functions for the transferred particle bound to the projectile or target. The no-recoil approximation is obtained by setting $\vec{r}_f = \alpha \vec{r}_i$ in $\Psi^{(-)}$. A more accurate procedure is to expand $\Psi^{(-)}$ in a series about $\alpha \vec{r}_i$.

From the exact relations

$$\vec{r}_f = \beta \vec{r}_i + \gamma \vec{r}_1, \quad \beta = \frac{M_B}{M_B + M_n}, \tag{3}$$

$$\gamma = \frac{(M_A + M_B + M_n) M_n}{(M_A + M_n)(M_B + M_n)},$$

we get

$$\vec{r}_f = \alpha \vec{r}_i + [(\beta - \alpha)\vec{r}_i + \gamma \vec{r}_i]. \tag{4}$$

If the transfer took place at a single point along the line joining the centers of target and projectile the no-recoil procedure would be sufficient. One then sees that reasonable values for α vary between β for transfer taking place at the center of the projectile to about $\beta + \gamma R_1/(R_1 + R_2)$ for transfer at the projectile surface. In the post version of DWBA the Woods-Saxon form for $V(\vec{r}_1)$ in Eq. (2) cuts off transfer much past this surface.

To improve on no-recoil we use Eq. (4) to expand $\Psi^{(-)}$ to first order as:

$$\Psi^{(-)}(\vec{r}_f) = \Psi^{(-)}(\alpha \vec{r}_i) + (\beta - \alpha) r_i \frac{\partial \Psi^{(-)}}{\partial (\alpha r_i)}(\alpha \vec{r}_i) + \gamma \frac{\vec{r}_1}{\alpha} \cdot \nabla_i \Psi^{(-)}(\alpha \vec{r}_i) \tag{5}$$

and insert the result in Eq. (2).

The first term of Eq. (5) leads to

$$I_{(0)}^{l_1 l_2 LM} = \sum_{m_1 m_2} \langle l_2 m_2 LM | l_1 m_1 \rangle \times \int d\vec{r}_i \, \Psi^{(-)*}(\vec{k}_f, \alpha \vec{r}_i) \times \mathcal{F}_{LM}^0(\vec{r}_i) \Psi^{(+)}(\vec{k}_i, \vec{r}_i), \tag{6}$$

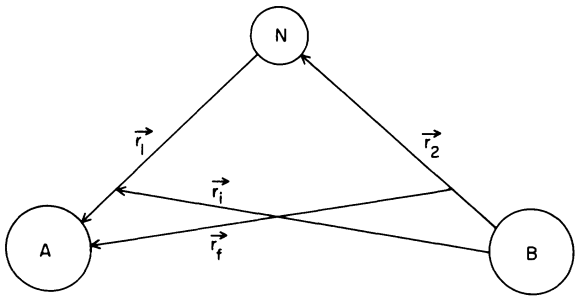

FIG. 1. Coordinates used in evaluating the DWBA integral.

where the no-recoil form factor is defined by

$$\mathcal{F}_{LM}^0(\vec{r}_i) = \sum_{m_1 m_2} \langle l_2 m_2 LM | l_1 m_1 \rangle \times \int d\vec{r}_2 \varphi_{j_2}^{l_2 m_2}(\vec{r}_2) V(\vec{r}_1) \varphi_{j_1}^{l_1 m_1}(\vec{r}_1). \tag{7}$$

A nonlocal form factor could have been introduced in the exact expression Eq. (2) by

$$\mathcal{F}_{LM}(\vec{r}_i, \vec{r}_f) = \sum_{m_1 m_2} \langle l_2 m_2 LM | l_1 m_1 \rangle \times \varphi_{j_2}^{l_2 m_2}(\vec{r}_2) V(\vec{r}_1) \varphi_{j_1}^{l_1 m_1}(\vec{r}_1), \tag{8}$$

whence the no-recoil result would follow from the ansatz

$$\mathcal{F}_{LM}(\vec{r}_i, \vec{r}_f) = \delta(\vec{r}_f - \alpha \vec{r}_i) \mathcal{F}_{LM}^0(\vec{r}_i). \tag{9}$$

It is clear a strong localization is imposed on $\mathcal{F}(\vec{r}_i, \vec{r}_f)$ by the cutoff form of interaction, and to a lesser degree by the target bound-state wave function. This localization to some extent justifies the above ansatz and thereby the no-recoil approximation.

The second term in Eq. (5), which vanishes when $\alpha = \beta$, can be calculated by a minor modification of a no-recoil code. We will investigate the third term in more detail:

$$I_{(1)}^{l_1 l_2 LM} = \frac{1}{\alpha} \sum_{m_1 m_2} \langle l_2 m_2 LM | l_1 m_1 \rangle \gamma \langle \vec{r}_1 \cdot \nabla_i \Psi^{(-)}(\alpha \vec{r}_i) \varphi_{j_2}^{l_2 m_2}(\vec{r}_2) | V(\vec{r}_1) | \varphi_{j_1}^{l_1 m_1}(\vec{r}_1) \Psi^{(+)}(\vec{r}_i) \rangle. \tag{10}$$

If we first write $\vec{r}_1$ in spherical coordinates

$$\vec{r}_1 = \sum_{\mu} (-1)^{\mu} r_1 (4\pi/3)^{1/2} Y_1^{\mu}(\hat{r}_1) \hat{\xi}_{-\mu}, \tag{11}$$

and use both the partial-wave expansion for $\Psi^{(-)*}$

$$\Psi^{(-)*}(\alpha \vec{r}_i) = 4\pi \sum_{l'm'} i^{-l'} Y_{l'}^{m'}(\hat{k}_f) Y_{l'}^{m',*}(\hat{r}_i) f_{l'}(\alpha r_i), \tag{12}$$

as well as the gradient formula[9]

$$\hat{\xi}_{-\mu}\cdot\nabla f_{l'}(\alpha r_i)Y_{l'}^{m'*}(\hat{r}_i)=(-1)^{m'}\left\{\left(\frac{l'+1}{2l'+3}\right)^{1/2}\langle l'-m'\,1-\mu\,|\,l'+1-m'-\mu\rangle\,Y_{l'+1}^{-m'-\mu}(\hat{r}_i)\left[\frac{df_{l'}(\alpha r_i)}{d(\alpha r_i)}-\frac{l'}{\alpha r_i}f_{l'}(\alpha r_i)\right]\right.$$
$$-\left(\frac{l'}{2l'-1}\right)^{1/2}\langle l'-m'\,1-\mu\,|\,l'-1-m'-\mu\rangle$$
$$\left.\times Y_{l'-1}^{-m'-\mu}(\hat{r}_i)\left[\frac{df_{l'}(\alpha r_i)}{d(\alpha r_i)}+\frac{l'+1}{\alpha r_i}f_{l'}(\alpha r_i)\right]\right\}, \tag{13}$$

we then obtain

$$\left(\frac{\gamma}{\alpha}\right)\vec{r}_1\cdot\nabla_i\Psi^{(-)*}(\alpha r_i)=4\pi\gamma\sum_{l'm'}i^{-l'}Y_{l'}^{m'}(\hat{k}_f)\sum_{\mu}(-1)^{\mu+m'}r_1(4\pi/3)^{1/2}Y_1^{\mu}(\hat{r}_1)$$
$$\times\left\{\left(\frac{l'+1}{2l'+3}\right)^{1/2}\langle l'-m'\,1-\mu\,|\,l'+1-m'-\mu\rangle\,Y_{l'+1}^{-m'-\mu}(\hat{r}_i)\right.$$
$$\times\left[\frac{df_{l'}(\alpha r_i)}{d(\alpha r_i)}-\frac{l'}{\alpha r_i}f_{l'}(\alpha r_i)\right]-\left(\frac{l'}{2l'-1}\right)^{1/2}\langle l'-m'\,1-\mu\,|\,l'-1-m-\mu\rangle$$
$$\left.\times Y_{l'-1}^{-m'-\mu}(\hat{r}_i)\left[\frac{df_{l'}(\alpha r_i)}{d(\alpha r_i)}+\frac{l'+1}{\alpha r_i}f_{l}(\alpha r_i)\right]\right\}. \tag{14}$$

The expression for $I_{(1)}^{l_1l_2LM}$ may now be written

$$I_{(1)}^{l_1l_2LM}=4\pi\gamma\sum_{l'm'\mu}i^{-l'}Y_{l'}^{m'}(\hat{k}_f)\int\left(\frac{M_A+M_n}{M_A}\right)^3d\vec{r}_i$$
$$\times\left[Y_{l'-1}^{m'+\mu*}(\hat{r}_i)\langle l'm'\,1\mu\,|\,l'-1m'+\mu\rangle\,D_{l'-1}(r_i)+Y_{l'+1}^{m'+\mu*}(\hat{r}_i)\langle l'm'1\mu\,|\,l'+1m'+\mu\rangle\,D_{l'+1}(r_i)\right]$$
$$\times F_{M\mu}^{L}(\vec{r}_i)\Psi^{(+)}(\vec{r}_i), \tag{15}$$

where

$$D_{l'+1}(r_i)=\left(\frac{l'+1}{2l'+3}\right)^{1/2}\left[\frac{df_{l'}(\alpha r_i)}{d(\alpha r_i)}-\frac{l'}{\alpha r_i}f_{l'}(\alpha r_i)\right], \tag{16}$$

$$D_{l'-1}(r_i)=-\left(\frac{l'}{2l'-1}\right)^{1/2}\left[\frac{df_{l'}(\alpha r_i)}{d(\alpha r_i)}+\frac{l'+1}{\alpha r_i}f_{l'}(\alpha r_i)\right] \tag{17}$$

are modified radial "wave functions," while

$$F_{M\mu}^{L}(r_i)=\sum_{m_1m_2}\int(4\pi/3)^{1/2}Y_1^{\mu}(\hat{r}_1)Y_{l_1}^{m_1}(\hat{r}_1)Y_{l_2}^{m_2*}(\hat{r}_2)\varphi_2(r_2)V(r_1)\varphi_1(r_1)r_1d\vec{r}_2\langle l_2m_2LM\,|\,l_1m_1\rangle \tag{18}$$

is a modified form factor.

$F_{M\mu}^{L}(r_i)$ may be evaluated by applying the identity

$$\vec{r}_1=\frac{M_A+M_n}{M_A}(\vec{r}_i-\vec{r}_2),$$

and then using the Sawaguri-Tobocman expansion to integrate over $\vec{r}_2$.[10] In particular we may write for arbitrary functions $\varphi_j(r_1)$ and $\varphi_k(r_2)$

$$\int Y_{l_k}^{m_k*}(\hat{r}_2)Y_{l_j}^{m_j}(\hat{r}_1)\varphi_k(r_2)\varphi_j(r_1)d\vec{r}_2=\sum_{L'}8\left[\frac{(2L'+1)(2l_j+1)}{4\pi(2l_k+1)}\right]^{1/2}\langle L'm_k-m_jl_jm_j\,|\,l_km_k\rangle$$
$$\times\langle L'0l_j0\,|\,l_k0\rangle\,Y_{L'}^{m_k-m_j*}(\hat{r}_i)\bar{F}_{L'}^{l_jl_k}(r_i). \tag{19}$$

Of course $\bar{F}_{L'}^{l_jl_k}(r_i)$ depends on the explicit radial form of $\varphi_k(r_2)$ and $\varphi_j(r_1)$ in addition to l_j, l_k, and L'. We use expression (19) by letting $\varphi_k(r_2)=\varphi_2(r_2)$ and $\varphi_j(r_1)=V(r_1)\varphi_1(r_1)r_1$.

Some tedious but straightforward Racah algebra must now be performed. The explicit partial wave ex-

pansion for the incoming channel is

$$\Psi^{(+)}(\vec{r}_i)=\sum_l i^l[4\pi(2l+1)]^{1/2}Y_l^0(\hat{r}_i)f_l(r_i) \tag{20}$$

for a quantization axis along the direction of the incoming beam. One obtains finally

$$I_{(1)}^{l_1l_2LM}=\gamma\left(\frac{M_A+M_n}{M_A}\right)^3\sum_{ll'\lambda l''} 8\left[\frac{(2l_1+1)(2l_2+1)}{4\pi(2L+1)}\right]^{1/2} i^{l-l'}(4\pi)^{3/2}Y_{l'}^{M}(\hat{k}_f)(-1)^{l_1-\lambda-M}\left[\frac{3(2l''+1)(2\lambda+1)}{4\pi(2L+1)}\right]^{1/2}$$
$$\times\langle l'ML-M|l0\rangle\langle l''0\lambda0|l0\rangle U(l'1l\lambda;l''L)\int dr_i r_i^2 C_\lambda(r_i)D_{l''}(r_i)f_l(r_i), \tag{21}$$

with

$$C_\lambda(r_i)=-\left(\frac{l_1}{3}\right)^{1/2}\langle l_20l_1-10|\lambda0\rangle U(l_1l_21\lambda;Ll_1-1)\bar{F}_\lambda^{l_1-1l_2}(r_i)+\left(\frac{l_1+1}{3}\right)^{1/2}\langle l_20l_1+10|\lambda0\rangle$$
$$\times U(l_1l_21\lambda;Ll_1+1)\bar{F}_\lambda^{l_1+1l_2}(r_i), \tag{22}$$

and $D_{l'+1}$ and $D_{l'-1}$ are defined in Eqs. (16) and (17).

Including recoil introduces additional transferred angular momenta. If spin-orbit forces in the scattering channels are ignored, the allowed L values are restricted by the triangular relations

$$|j_1-j_2|<L<|j_1+j_2|$$

and

$$|l_1-l_2|<L<|l_1+l_2|.$$

In the no-recoil approximation the additional parity restriction $(-1)^{l_1+l_2+L}=1$ applies, leading to so-called normal L values. This restriction disappears in the full-recoil calculation; the additional allowed L values are then referred to as nonnormal. This is evident from inspection of Eqs. (21) and (22). If $M=0$ for a nonnormal L the parity restriction still holds and the corresponding amplitude vanishes, at least within our coordinate framework.

III. CODING AND CONVERGENCE

The resultant first-order recoil formalism has been coded as a modification of the existing no-recoil code RDRC.[4] We will call the modified code FRC (first-order recoil code). The coding was checked by comparison with an analytical calculation employing plane-wave scattering states $\Psi^{(\pm)}$ and oscillator bound states $\varphi_{1,2}$. A typical calculation with our code takes some 3 or 4 times longer than the corresponding calculation with RDRC. Half the increase in time results from the additional, nonnormal, angular-momentum transfers. It is then quite practical to analyze data with this code, provided one is considering a case for which the present procedure is convergent.

Some estimate of the degree of convergence may be obtained by examining Eqs. (5) and (14). One can write Eq. (5) in the form

$$\Psi^{(-)}(\vec{r}_f)=\exp\{i[\gamma\vec{r}_1+(\beta-\alpha)\vec{r}_i]\cdot\nabla_i\}\Psi^{(-)}(\alpha\vec{r}_i). \tag{23}$$

In a local-momentum approximation $\nabla_i\to\vec{k}_i(\alpha\vec{r}_i)$ and our procedure then reduces to an expansion of the exponential in Eq. (23)

$$\exp\{i[\gamma\vec{r}_1+(\beta-\alpha)\vec{r}_i]\cdot\vec{k}_i\}$$
$$=1+i\vec{k}_i\cdot[\ ]+\tfrac{1}{2}(i\vec{k}_i\cdot[\ ])^2+\cdots. \tag{24}$$

When $\vec{k}_i\parallel\vec{r}_i$ radial derivatives of the scattering wave function are relevant and one might take

$$|\vec{k}^{\,\text{radial}}|=\left([E-U(\vec{r}_f)-V_C(\vec{r}_f)]-\frac{\hbar^2l(l+1)}{2\mu_f r_f^2}\frac{2\mu_f}{\hbar^2}\right)^{1/2},$$

where U is the real optical potential and V_C the Coulomb potential in the exit channel. For the grazing l_0 one expects transfer to be strongest at or near the distance of closest approach where $|k_i^{\text{radial}}|\approx0$. This suggests the radial derivative terms in Eq. (14) may be small. The remaining terms in Eq. (14) result from angular derivatives, i.e., $\vec{k}_i\perp\vec{r}_i$; for these clearly $|\vec{k}^{\perp}|\simeq\{[E-U(\vec{r}_f)-V_C(\vec{r}_f)](2\mu_f/\hbar^2)\}^{1/2}$. Since we expect transfer to take place reasonably near the Coulomb barrier, i.e., where $(d/dr_f)(U+V_C)=0$, the local momentum $k^{\perp}$ is considerably decreased from $k_\infty=(2\mu E/\hbar^2)^{1/2}$. This aids convergence. A crude estimate of the expected accuracy can be obtained by examining the second-order term in Eq. (24) which, for $\alpha=\beta$, is $\frac{1}{2}\gamma^2(\vec{k}\cdot\vec{r}_1)^2$. Using the above arguments for $k^{\perp}$, $k^{\parallel}$ and averaging over the "angle" between $\vec{k}_i$ and $\vec{r}_1$, we are led to

$$\langle\tfrac{1}{2}\gamma^2(\vec{k}\cdot\vec{r}_1)^2\rangle\approx\tfrac{1}{6}\gamma^2(E-U-V_C)\frac{2\mu}{\hbar^2}r_1^2$$

$$\approx\frac{1}{3}\ \frac{M_n}{\mu\hbar^2}(E-U-V_C)r_1^2.$$

For projectiles like ^{16}O, ^{13}C, $r_1 \sim 2.5$–3 fm and we deduce a second-order term $\sim (E - E_{\text{barrier}})/15\mu$. This calculation gives only a crude guide to the region of validity of our first-order estimate; clearly the approximation will break down at energies sufficiently above the barrier.

Perhaps a better indication of the convergence of our code may come from examining the dependence on the "hidden" parameter α. An exact expansion of the power series must lead to a result independent of this parameter. The extent to which this is accomplished by a truncated series should give an indication of the degree of convergence. Later we will quote results indicating the first-order calculation satisfies this criterion to a surprising extent. It is, in fact, impossible to uniquely state the effect of recoil on the reaction cross section without fixing a value for α. In general, for a projectile considerably lighter (and therefore smaller) than the target nucleus, one finds the α dependence much stronger in the prior rather than in the post representation of the amplitudes. This suggests recoil corrections are larger in the prior form, as indeed one might expect from the large value of $(\vec{r}_2)$ to be inserted in expression of $e^{\gamma \vec{r}_2 \cdot \nabla_i}$ in Eq. (23).

IV. APPLICATION

To illustrate our approach we examine two one-nucleon transfer experiments performed at the Brookhaven National Laboratory tandem Van de Graaff facility, $^{94}Mo(^{13}C, ^{12}C)^{95}Mo$ and ^{48}Ca-$(^{14}N, ^{13}C)^{49}Sc$ at laboratory energies of 48.5 and 50 MeV, respectively. The results of a theoretical analysis of these reactions is reported elsewhere.[11–13] Of interest here are the effects of recoil, which were referred to but not described in detail in this earlier work. The above reactions and energies were chosen because of contrasting angular distributions obtained. The neutron transfer reaction occurs at an energy just above the barrier and exhibits a semiclassical bell-shaped angular distribution, while the proton transfer occurs just below twice the barrier energy and exhibits a strong diffractive and forward angle structure. A qualitative picture encompassing both these shapes is given in Ref. 13.

The results of no-recoil calculations and those done with the first-order recoil code described above do not differ appreciably in shape for a given angular-momentum transfer L. This is illustrated in Fig. 2 where no-recoil computations for ^{48}Ca-$(^{14}N, ^{13}C)$ to the ^{49}Sc $(1f_{7/2})$ ground state and $(2p_{3/2})$ 3.08-MeV state are compared with normal L results with recoil. In the case of the ground state of ^{49}Sc the normal parity transfer is for $L=4$. At an

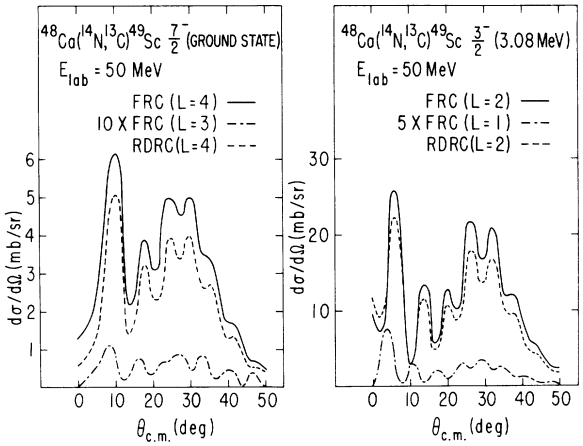

FIG. 2. Comparison of no-recoil (RDRC) and first-order recoil (FRC) computed angular distributions for $^{48}Ca(^{14}N, ^{13}C)^{49}Sc$.

energy of 50 MeV transfer is dominated by the magnetic quantum states $M=\pm 4$ for quantization along the incoming beam direction. This results in the most forward peak in the angular distribution occurring at an angle $> |M|/l_0 = 4/l_0$ and subsequent peaks at angles determined from $\sin[(2l_0+1)\theta_{\max}] = 1$, where l_0 labels the outgoing partial wave for which transfer is strongest.[13] The nonnormal parity transfer is for $L=3$ in the ground-state transfer which is again dominated by the maximum $|M|=3$; an odd value which leads to peaks in the angular distribution at $\sin(2l_0+1)\theta = -1$.

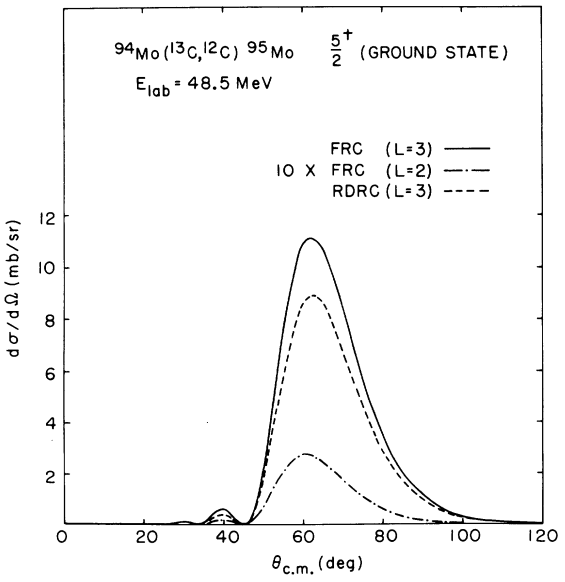

FIG. 3. Comparison of no-recoil (RDRC) and first-order recoil (FRC) computed angular distributions for $^{94}Mo(^{13}C, ^{12}C)^{95}Mo$.

TABLE I. Absolute magnitudes of peak cross sections calculated with RDRC and FRC. Under S are the spectroscopic factors extracted from the heavy-ion-induced transfer data.

Reaction	E	J^π	L	σ_{RDRC}	σ_{FRC}	S	$S(d,p)$
^{94}Mo(^{13}C, ^{12}C)^{95}Mo	0	$\frac{5}{2}^+$	3	8.88	11.10	0.59	0.59
			2		0.28		
	0.821	$\frac{3}{2}^+$	1	2.59	3.05	$\leq$0.14	0.255
			2		0.59		
		$\frac{5}{2}^+$	3	11.43	14.07	$\leq$0.03	0.17
			2		0.39		
^{48}Ca(^{14}N, ^{13}C)^{49}Sc	0	$\frac{7}{2}^-$	4	5.03	6.48	0.67	1
			3		0.10		
		$\frac{5}{2}^-$	2	1.07	0.82		
			3		0.14		
	3.08	$\frac{3}{2}^-$	2	20.3	24.8	0.36$\pm$0.06	$\sim$0.6
			1		0.75		
		$\frac{1}{2}^-$	0	5.75	8.13		
			1		1.50		

Thus the normal and nonnormal transfers in this situation are both oscillatory (see Fig. 2) but just out of phase. Should the nonnormal transfer be large quite evident changes in oscillating angular distribution would result. For the present one-proton reaction the nonnormal transfer is not appreciable to either the ground $f_{7/2}$ or 3.08-MeV $p_{3/2}$ states.

In a case which is clearly a smooth "grazing" angular distribution such as ^{94}Mo(^{13}C, ^{12}C) at 48.5 MeV the angular shape shows almost no dependence on L; no recoil and recoil, normal and nonnormal, are essentially indistinguishable (Fig. 3).

We have presented our calculations in various other forms. In Table I we consider the prediction of absolute cross-section magnitudes by comparing the experimental data obtained at specific laboratory energies with calculations indicating separately the no-recoil, normal, and nonnormal recoil results. For the relatively low-energy neutron transfer we simply quote peak cross section, whereas for the oscillatory proton transfer we use total cross section as a measure of magnitude. If the necessary (^{13}C, ^{12}C) and (^{14}N, ^{13}C) spectroscopic factors are taken from Cohen and Kurath[14] then spectroscopic factors may be estimated for the ^{95}Mo and ^{49}Sc states. These compare well with spectroscopic information extracted from known light-projectile transfer.[11-13,17,18] Including recoil corrections is significant for all states considered but especially important for $j_1 = l_1 - \frac{1}{2}$ final states. Semiclassical arguments suggest that at low energy the incoming bound particle in a $1p_{1/2}$ ($j_1 = l_1 - \frac{1}{2}$) will be favorably transferred into a $j_2 = l_2 + \frac{1}{2}$ rather than a $j_2 = l_2 - \frac{1}{2}$ final state in the target. This feature is borne out in the calculations and was used to identify the spin of a 0.821-MeV state[11] in analyzing ^{95}Mo final-state data.

The j and Q dependence of the recoil corrections are best understood by performing theoretical experiments, rather than by comparison with specific data. In Table II and Fig. 4 we explore these dependences for two j pairs of levels, ($2p_{1/2}$, $2p_{3/2}$) and ($1f_{5/2}$, $1f_{7/2}$), appropriate to the single-proton transfer ending in ^{49}Sc. Table II indicates the energy dependence of the ratios $\sigma_>/\sigma_<$. In each case the transferred particle is initially bound in a $1p_{1/2}$ state in the projectile. The previously used semiclassical argument suggests as the energy increases the $j = l + \frac{1}{2}$ state should be less favored relative to the $j = l - \frac{1}{2}$ final state. This argument depends, however, on a proper treatment of recoil. Table II indicates the ratio $\sigma_>/\sigma_<$ generally decreases more with energy when our first-order recoil correction is included. A point of interest in Table II is the decrease produced at 30 MeV in the $f_{5/2}$ cross section when recoil is in-

TABLE II. Total cross sections (in mb) for $j_>$ and $j_<$ states in ^{48}Ca(^{14}N, ^{13}C)^{49}Sc as a function of incident projectile energy.

j^p \ E		30	50	70
$\frac{7}{2}^-$	(FRC)	4.03	6.48	6.22
	(RDRC)	3.76	5.03	4.88
$\frac{5}{2}^-$	(FRC)	0.253	0.818	1.35
	(RDRC)	0.455	1.07	1.20
$\sigma_>/\sigma_<$	(FRC)	15.9	7.92	4.61
	(RDRC)	8.26	4.70	4.07
$\frac{3}{2}^-$	(FRC)	28.4	24.8	20.4
	(RDRC)	23.9	20.3	17.6
$\frac{1}{2}^-$	(FRC)	7.15	8.13	7.60
	(RDRC)	6.24	5.75	4.43
$\sigma_>/\sigma_<$	(FRC)	3.97	3.05	2.68
	(RDRC)	3.83	3.53	3.97

cluded. In this table both $1f$ states are calculated at the $\frac{7}{2}^-$ ground-state Q value and both $2p$ states are calculated at the 3.08-MeV excited state for ^{49}Sc.

Perhaps the most revealing manner in which to display this comparison is indicated in Figs. 4 and 5 where the no-recoil and first-order recoil total cross sections are plotted as a function of excitation energy [$= Q(\text{g.s.}) - Q$]. The cross sections calculated at laboratory energies of 50 and 30 MeV for the reaction ^{40}Ca(^{14}N, ^{13}C) are shown in Figs. 4 and 5. Both $j_<$ states exhibit crossovers, with recoil values being sometimes larger, sometimes smaller than no-recoil. Some care must then be taken in using a no-recoil analysis to extract structure information for $j_<$ states. On the other hand, the $j_>$ states are well described by the no-recoil approximation over a wide range of Q values or excitation energies.

The optimum or peak Q values for the $j_>$ states

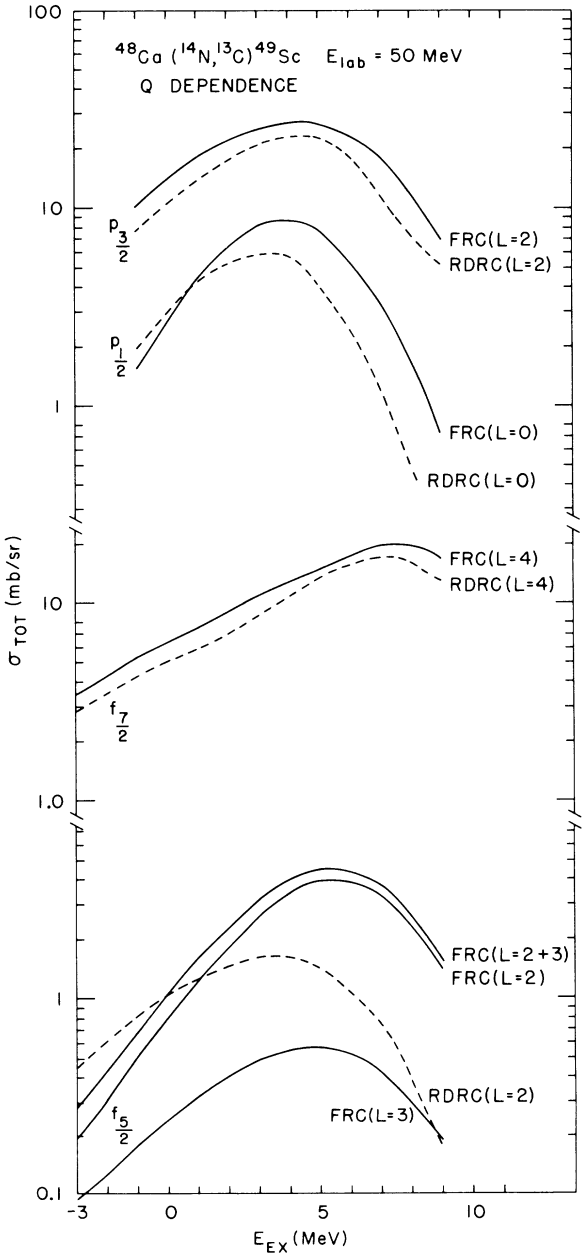

FIG. 4. Q dependence of computed cross sections for ^{48}C(^{14}N, ^{13}C)^{49}Sc at 50 MeV.

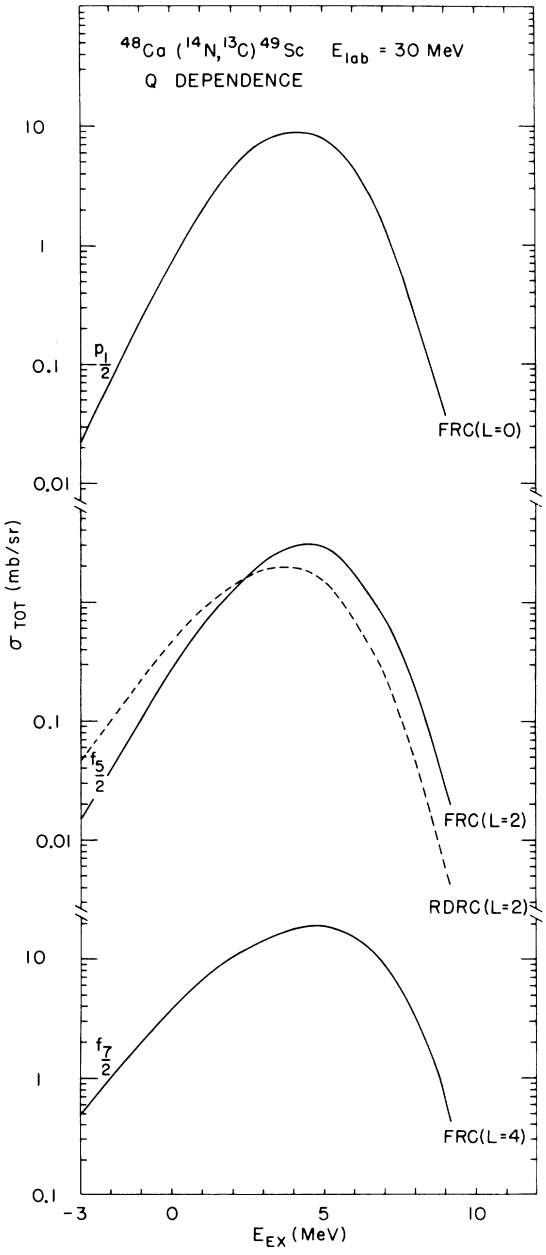

FIG. 5. Q dependence of computed cross sections for ^{48}Ca(^{14}N, ^{13}C)^{49}Sc at 30 MeV.

TABLE III. Dependence of ^{48}Ca(^{14}N, ^{13}C)^{49}Sc calculated cross sections as a function of the scaling parameter α at 50 MeV.

		RDRC		FRC	
		$\alpha=0.98$	$\alpha=1.01$	$\alpha=0.98$	$\alpha=1.01$
$(\frac{7}{2}^-)$	30°	3.95	4.61	4.99	5.04
	24°	3.86	4.65	4.96	4.99
$(\frac{3}{2}^-)$	32°	16.77	21.29	20.83	22.22
	26°	17.70	22.42	21.60	23.05

in both Figs. 4 and 5 are reasonably well described by the classical relations[15,16]

$$Q = U_f - U_i + \frac{mv^2}{2} - \lambda_2 \frac{\hbar v}{r_2}$$

$$= U_f - U_i - \frac{mv^2}{2} + \lambda_1 \frac{\hbar v}{r_1},$$

$$\hbar\left(\frac{\lambda_1}{r_1} + \frac{\lambda_2}{r_2}\right) = mv, \tag{25}$$

where U_i, U_f are the real optical potentials at positions of transfer in the entrance and exit channels, v is the local relative velocity at transfer, r_1 and r_2 are radial distances of the transferred particle from projectile and target, and λ_1, λ_2 the projections of angular momentum for the transferred-particle orbits in a direction perpendicular to the plane of motion at transfer. The choice of λ_1, λ_2 is somewhat ambiguous. At 30-MeV laboratory energy, ^{14}N ions incident on ^{48}Ca are just about at the Coulomb barrier and we expect $v \to 0$ and $Q = U_f - U_i \approx 2.2$ MeV for all four states $f_{7/2,5/2}$, $p_{3/2,1/2}$. The curves in Fig. 5 confirm this state independence and all exhibit a maximum near $E_{\text{excitation}} = +Q_{\text{g.s.}} + 2.2 = 4$ MeV. Clearly recoil plays little role in the Q curves of Fig. 5 as one expects. It is only possible to crudely analyze the $j_>$ curves at 50 MeV in a manner consistent with Eqs. (25), also differences between $j_<, j_>$ are not included in the classical relations. The increased role of recoil is evident at 50 MeV; there is a more noticeable shift between recoil and no-recoil values for the optimum Q. The slower dependence of cross section on Q at 50 MeV, for say the $f_{7/2}$ curve, makes the classical concepts less useful at this higher energy.

Convergence and α dependence

Perhaps the most unsatisfactory feature of the no-recoil approximation is the presence of the scaling parameter α. We have argued a physical range is $\beta < \alpha < \beta + \gamma R_1/(R_1 + R_2)$. Our approach to including recoil builds on no-recoil and necessarily retains some dependence on α. In this section we would like to argue that to a considerable degree the first-order recoil calculation eliminates or greatly reduces the unwanted dependence. We have also previously argued the independence from α is a sign of convergence. Table III and Fig. 6 summarize the results of exploratory calculations again on the (^{14}N, ^{13}C) transfer. Table III considers α dependence of $1f_{7/2}$ and $1p_{3/2}$ states at experimentally observed excitation energies (0 and 3.08 MeV).

In every case the variation of cross section with α is reduced appreciably by the first-order recoil. One might, in fact, use the remaining variation in cross section as an estimate of error in our calculations; thus $f_{7/2}$ (30°) is expected to be accurate to ~1% and $p_{3/2}$ (32°) to ~7% or so. A more striking display of this information is obtained by replotting the Q curve of Fig. 6 for the $f_{5/2}$ final state. For this particular state and a 50-MeV incoming ^{14}N projectile we have the greatest calculated discrepancy between no-recoil and first-order recoil. Nevertheless, with extreme choices for α in the

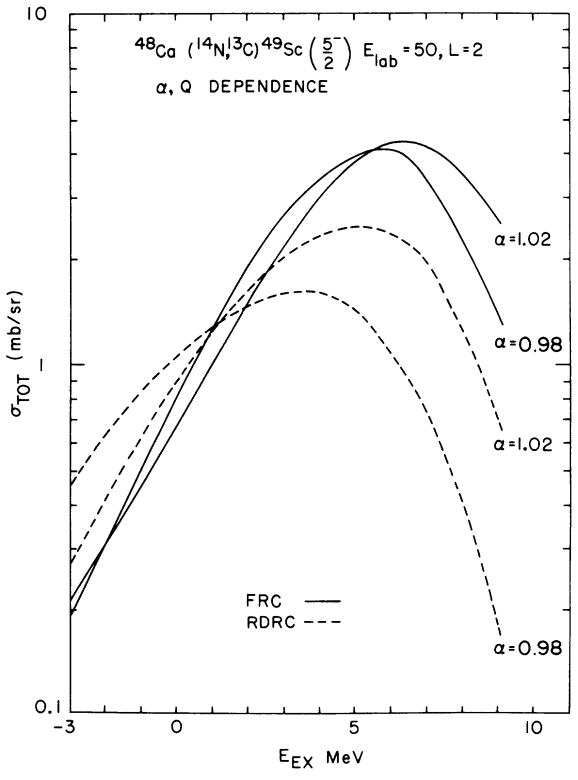

FIG. 6. Q dependence of ^{48}Ca(^{14}N, ^{13}C)^{49}Sc $(\frac{5}{2}^-)$ at 50 MeV for two values of the scaling parameter α. The $(\frac{5}{2}^-)$ state shown has the largest differences between no-recoil (RDRC) and first-order (FRC) calculations. Note that FRC calculations are relatively α-independent over a broad Q range.

expected range, the two recoil calculations shown in Fig. 6 track each other surprisingly well with Q. We take this as a strong indication of convergence for our series approach at these energies.

CONCLUSIONS

The present code is ideally suited for use in the analysis of experimental data. It consumes approximately twice the time of a no-recoil code for a given angular-momentum transfer and apparently converges well over a wide range of Q values and projectile energy. The clearest evidence for convergence is the degree to which independence from the scaling parameter α is achieved (Fig. 6). Ideally, this should be checked by comparison with results of formally more complete approaches. What has been done so far indicates good agreement with "in-principle" exact quadrature of the finite-range transfer. For example in the reaction $^{88}Sr(^{16}O, ^{15}N)$ to the $p_{1/2}$ ground and $g_{9/2}$ excited states of ^{89}Y at energies from 42.5 to 59 MeV (lab) over-all peak cross sections differ by no more than 7% whereas recoil corrections are at least four times larger.[8]

The authors would very much like to thank P. D. Bond and J. D. Garrett for help in preliminary use and debugging of FRC.

---

*Work performed under the auspices of the U.S. Atomic Energy Commission.

[1]H. J. Körner, G. C. Morrison, L. R. Greenwood, and R. H. Siemssen, Phys. Rev. C 7, 107 (1973).
[2]F. D. Becchetti, P. R. Christensen, V. I. Manko, and R. J. Nickles, Phys. Lett. B43, 279 (1973).
[3]E. H. Auerbach, A. J. Baltz, P. D. Bond, C. Chasman, J. D. Garrett, K. W. Jones, S. Kahana, M. J. LeVine, M. Schneider, A. Z. Schwarzchild, and C. E. Thorn, Phys. Rev. Lett. 30, 1678 (1973).
[4]F. Schmittroth, W. Tobocman, and A. A. Golestaneh, Phys. Rev. C 1, 377 (1970).
[5]R. De Vries and K. Kubo, Phys. Rev. Lett. 30, 325 (1973).
[6]C. MacLaurin, *A Treatise of Fluxions* (Edinburgh, 1742).
[7]M. A. Nagarajan, Nucl. Phys. A196, 34 (1972).
[8]J. Blair, R. M. DeVries, A. J. Baltz, G. Nair, and W. Reisdorf (to be published).
[9]M. E. Rose, *Multipole Fields* (Wiley, New York, 1955).
[10]T. Sawaguri and W. Tobocman, J. Math. Phys. (AIP) 8, 2223 (1967).
[11]P. D. Bond, C. Chasman, M. W. LeVine, A. Z. Schwarzschild, C. E. Thorn, and A. J. Baltz, Phys. Rev. C 9, 2001 (1974).
[12]M. J. Schneider, C. Chasman, E. H. Auerbach, A. J. Baltz, and S. Kahana, Phys. Rev. Lett. 31, 320 (1973).
[13]C. Chasman, S. Kahana, and M. J. Schneider, Phys. Rev. Lett. 31, 1074 (1973).
[14]S. Cohen and D. Kurath, Nucl. Phys. A101, 1 (1967).
[15]D. M. Brink, Phys. Lett. 40B, 37 (1972).
[16]S. Kahana, in Symposium on Heavy-Ion-Transfer Reactions, Argonne, 1973, Vol. I, 385.
[17]G. Bruge, H. Faraggi, H. Duc Long, and P. Ronssel, Commisariat à l'Energie Atomique Report No. CEA-N 1232, 1970 (unpublished), p. 124.
[18]J. B. Moorhead and R. A. Moyer, Phys. Rev. 184, 1205 (1969).